Interpretation of substrate photoelectron diffraction

S. Hüfner,* J. Osterwalder, T. Greber, and L. Schlapbach
Institut de Physique, Université de Fribourg, CH-1700 Fribourg, Switzerland
(Received 7 March 1990; revised manuscript received 12 June 1990)

Azimuthal diffraction patterns of 1*s* and 2*s* photoelectrons, of plasmon-loss peaks and inelastic-background intensities, as well as of medium-energy electrons, are presented for polar angles of 45° and 55° off the surface normal of a clean Al(001) crystal. A comparison of such data is important for the assessment of two currently used models for describing electron diffraction: the short-range scattering-cluster approach and the Kikuchi or Bragg-scattering method. It is concluded that both methods are essentially equivalent. Differences in experimental diffraction patterns of elastically and inelastically scattered electrons can be related to different probing depths and, associated with it, different relative importance of multiple scattering. It is also found that photoelectron-diffraction patterns and medium-energy electron-diffraction patterns in the 1-keV regime are very similar, as long as the kinetic energies are not too different. From this it follows that substrate photoelectron-diffraction patterns can be more easily obtained by elastic electron scattering.

INTRODUCTION

In a photoelectron-diffraction experiment, the electrons are photoemitted from a single-crystal surface and then detected under varying geometrical conditions.[1,2] Thereby the diffraction of the photoelectrons by the surface region of the sample can be measured and used to obtain structural information. These experiments can be performed either by scanning the energy of the exciting radiation, i.e., the wavelength of the emitted electrons, at a fixed electron detection geometry, or by scanning the azimuthal and polar angles under which the electrons are detected, keeping the exciting radiation at a fixed energy. This latter mode is generally applied if x rays are employed [x-ray photoelectron diffraction (XPD)], and strong modulations in the photocurrent are observed, with anisotropies of up to 70%. Similar angular diffraction patterns can also be measured with Auger electrons[3,4] and with quasielastically backscattered medium-energy electrons.[5–7] Moreover, it has been noticed already some time ago that Kikuchi electrons as produced, e.g., in a low-energy electron-diffraction (LEED) experiment, show essentially the same diffraction patterns as Auger electrons.[3] Kikuchi electrons are electrons which are inelastically scattered from a primary beam of monoenergetic electrons. It is commonly agreed that the Kikuchi patterns arise because the inelastically scattered electrons are Bragg reflected off low-index crystal planes before they leave the crystal. Considering the similarities in all of these diffraction patterns, it seems that the underlying mechanism must be the same for photoelectrons, Auger electrons, backscattered medium-energy electrons, and Kikuchi electrons.

The analysis of diffraction patterns associated with photoelectrons and Auger electrons is very often and quite successfully done by means of single-scattering calculations.[1,2] In this method it is assumed that a photoelectron wave is generated at a lattice site and then scattered by all the ions within a restricted cluster. The interference between the primary wave and all the scattered waves produces the diffraction patterns. A key element in these calculations is the fact that the elastic-scattering cross sections for the energies under consideration (200–1500 eV) are strongly peaked in the forward direction. This leads to large peaks in the diffraction patterns whenever emission along densely packed rows of atoms is detected, as is illustrated, e.g., by dominant peaks along ⟨011⟩ directions in Auger electron diffraction from (001) surfaces of fcc crystals.[4]

A number of questions bearing upon the interpretation of electron-diffraction data are still under discussion. (i) Are the long-range Bragg scattering approach to Kikuchi patterns and the short-range scattering-cluster approach to photoelectron diffraction equivalent? (ii) Do photoelectron-diffraction data mainly show effects of rows of atoms in the crystal (via the strong forward scattering) or do they further contain truly diffractional patterns? If so, how can those be distinguished from the purely geometrical forward-scattering peaks? (iii) How important are multiple-scattering effects in the formation of XPD patterns?

We think that the answer to the first question has in principle already been given by Schaich,[8] to the effect that a short-range scattering-cluster calculation and a long-range Bragg-type diffraction calculation are in principle equivalent. However, from a comparison with simple two-beam Kikuchi profiles, it seems that scattering-cluster calculations are easier to get to converge than Bragg-scattering calculations, and are therefore preferable from a practical point of view.[9] Nevertheless, we think it could be worthwhile to apply the more-developed theory of Kikuchi diffraction patterns[10] to photoelectron diffraction. From the experimental point of view it should be emphasized that two investigations have explicitly noted the equivalence of Auger and Kikuchi diffraction patterns.[3,11]

In order to address the second question, a simple way for separating the true diffraction features from zero-

order forward-scattering-related peaks in a photoelectron-diffraction diagram is proposed: Diffraction patterns from a crystal surface are measured twice under the same experimental conditions except for changing the wavelength (kinetic energy) of the electrons. The true diffraction features will change shape and positions while the strictly geometrical patterns will remain more or less unchanged. A case in point here is a comparison of azimuthal photoelectron-diffraction data from the (001) surface of Al as measured with the 2*s* line ($E_B = 118$ eV) and the 1*s* line ($E_B = 1560$ eV) at a polar angle of 45°. These experiments show that only the strong intensities along the ⟨011⟩ directions are created by geometrical scattering, while all the other features, although weaker, are probably due to true diffraction.[12]

The answer to the third question can implicitly yield another method to distinguish geometrical features from true diffraction features. Xu *et al.*[13] have recently found that multiple scattering along rows of atoms spaced a few angstroms apart lead to a defocusing of the electron beams, thus effectively weakening the forward-scattering signals from emitters further below the surface. In particular, they presented calculations for the case of [011] nearest-neighbor rows in Cu at a kinetic energy of 1000 eV, showing that a row of four atoms following a source atom are enough to destroy the forward-scattering maximum along this direction completely. This then means that, if one makes an electron-diffraction experiment with electrons that are produced sufficiently deep in the crystal, one should observe only true diffraction features because the forward-scattering peaks are suppressed by multiple scattering.

While one has then an approximate understanding of the three questions raised above, detailed answers are still missing. It is the intention of this paper to deepen somewhat our understanding of XPD using new experiments from an Al(001) single crystal as a test case. The choice of this material has been made by realizing that it is about the only nearly-free-electron metal for which one can obtain high-quality single crystals that are relatively easy to clean. Nearly-free-electron metals have some advantages over the more commonly used transition metals, such as a simpler electronic structure[14–16] and well-developed plasmon losses,[17] which allow us to vary in a semiquantitative way the depth from which the measured photoelectrons were emitted.

The experimental details have been described in previous works and will therefore not be reported here.[12,18]

RESULTS AND DISCUSSION

XPD in the inelastic-loss spectrum

We now address questions (ii) and (iii) from above dealing with the relative importance of forward scattering and true diffraction features and with the significance of multiple-scattering effects in the formation of XPD patterns. As we shall see, these two problems are intimately related and therefore a joint discussion is justified.

If multiple-scattering effects are important in XPD, a measured XPD pattern should depend drastically on the depth from which the diffracted electrons originate. We have recently measured azimuthal diffraction curves of the Al 2*s* line and the first, second, and third associated plasmon-loss peaks.[12] The curves exhibit strong differences, with the forward-scattering maxima along ⟨011⟩ directions being gradually attenuated with increasing plasmon number. Assuming a total inelastic mean free path of 20 Å, and provided that plasmon creation does not destroy the coherence of the photoelectron wave, this led us to estimate the defocusing length, i.e., the distance at which the forward-scattering signal along rows of atoms gets completely suppressed, to be of the order of 45 Å, which is longer than believed up to now.

In this paper we take a more radical approach, which is illustrated in Fig. 1. The energy window for measuring XPS patterns is set at a kinetic energy 90 eV below the main 2*s* line (indicated as window II). There is no more structure in the energy spectrum this far below the main line and therefore it was decided to record the total inelastic intensity as indicated in Fig. 1. In order to measure the 2*s* line in a consistent manner, the window was set as indicated in Fig. 1 by window I. Note that this is an unusual way of recording XPD curves for a core line, because generally the background is subtracted by some suitable procedure. It is thus to be remembered that the integrated total intensities contain electrons with very different origins. In window I a large part will be true 2*s* photoelectrons together with some inelastically scattered 2*p* photoelectrons. It is not surprising that the azimuthal intensity scan recorded in window I at a polar angle of 45° (Fig. 2, upper curve) is essentially identical to the curve reported earlier[12] using a background subtraction. The overall anisotropy is naturally reduced from 65 to 48 % due to a more isotropic background contribution. We observe the expected fourfold symmetry of a fcc (001) surface, with maxima corresponding to electron detection along ⟨011⟩ directions. Along these directions one has

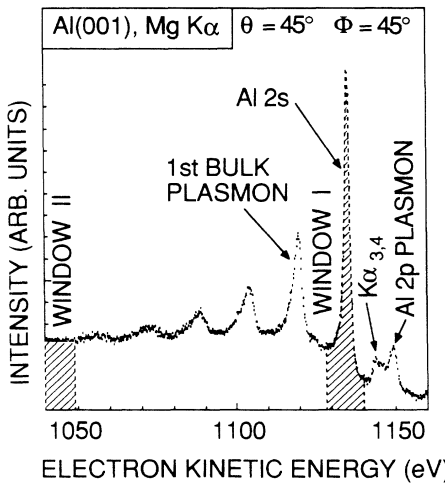

FIG. 1. Al 2*s* energy spectrum from Al(001), showing the main line and five plasmon-loss lines, measured along the low-symmetry direction $\Delta\phi = 45°$ off [011] using Mg $K\alpha$ radiation. Shaded areas indicate the energy windows used for obtaining the data in Fig. 2, i.e., with no background subtracted.

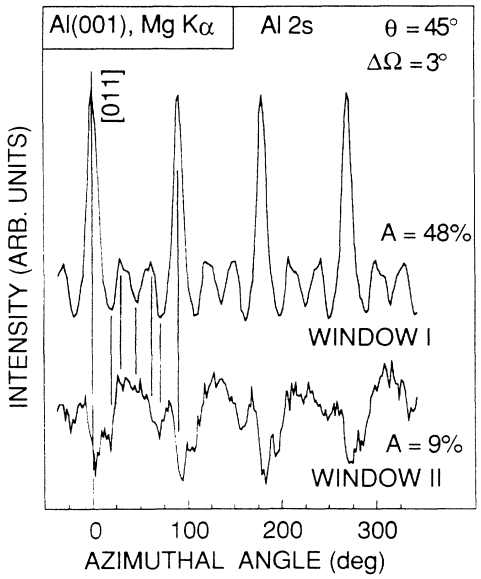

FIG. 2. Azimuthal intensity scans from Al(001) at a polar angle of $\theta=45°$ off normal, measured as indicated in Fig. 1. The two curves have been measured concurrently, i.e., the angle settings are identical and relative shifts of features such as along [011] are real.

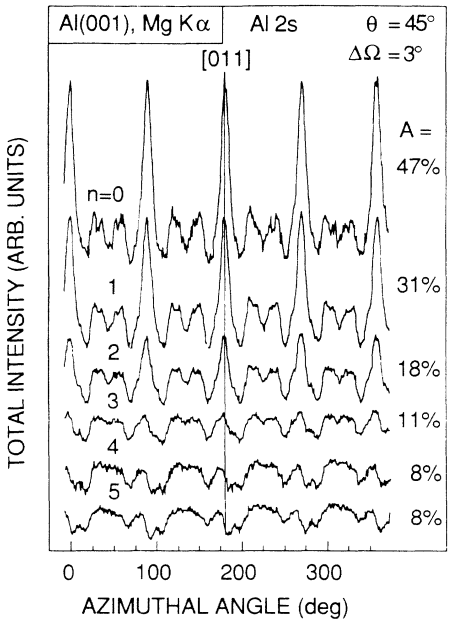

FIG. 3. Azimuthal intensity scans at $\theta=45°$, measured in the Al 2*s* no-loss line ($n=0$) and the consecutive plasmon-loss lines ($n=1$ through 5), using energy windows 15 eV apart and no background subtraction. Again, different curves have been measured concurrently, and relative peak shifts are real.

densely packed rows of atoms, and the large forward-scattering cross section produces these maxima.

The pattern measured in window II, which is produced by inelastically scattered electrons from various origins, is drastically different from that seen in window I, but there are still noticeable anisotropies observed. Since a good portion of the electrons in window II can be termed Kikuchi electrons, for which diffraction effects are well known to occur, the observation of an anisotropy in window II as such should present no surprise. However, the considerable difference in the XPD patterns is somewhat unexpected because it has been stated previously that photoelectrons (in the main core line) and Kikuchi electrons should show quite similar XPD patterns if the kinetic energies are not too different,[11] which clearly is not the case here. In addition, Mosser *et al.*[19] find only very weak diffraction effects in the Kikuchi electron angular distribution from Al for a loss of 100 eV, which is close enough to the present loss energy of 90 eV to make a meaningful comparison.

Figure 3 shows the development of the 2*s* core-level XPD in the Kikuchi patterns by comparing several measurements with energy decrements of 15 eV, which corresponds to the plasmon-loss energy of Al. Intensities were always evaluated consistently in the same way as indicated in Fig. 1, i.e., no background correction was performed. These data show the same trend as observed previously in an XPD investigation of the background-subtracted plasmon-loss peaks:[12] The dominant intensity maxima along the ⟨011⟩ directions decrease with the increasing energy separation of n times 15 eV from the main line. The number n of plasmon excitations by a photoelectron can be viewed as a measure of the depth of its origin. The longer an electron has to travel through the crystal lattice before leaving the surface, the more important multiple-scattering effects will be. It is therefore the well-known defocusing by multiple scattering[13,20] that leads to the suppression of these forward-scattering signals.

For Al the main energy-loss process for electrons with a kinetic energy of 1000 eV is plasmon scattering, with $\hbar\omega_p=15$ eV.[17] An energy loss of 90 eV corresponds therefore to an inelastic-scattering interaction with six plasmons. If one now assumes that the plasmon-scattering mean free path equals the total escape depth (actually it is somewhat longer[15]), such electrons come from a depth of typically 6×20 Å, which is an accepted value for the escape depth in Al at 1000 eV.[21] Therefore electrons at 90 eV below the main 2*s* line of Al ($E_B=118.0$ eV) excited with Mg $K\alpha$ radiation ($h\omega=1253.6$ eV) come from a region at least 100 Å below the surface, corresponding to about 50 atomic layers in Al with a lattice constant of 4.02 Å. Consequently, such electrons should show no forward-scattering features due to geometrical rows of atoms, whereas Bragg-like Kikuchi patterns should still be visible.

The XPD patterns measured in the background more than 60 eV away from the main 2*s* line ($n\geq4$) are distinctly different from that obtained with the core line, while of course the fourfold symmetry is retained. A very noteworthy observation in the data of Fig. 3 is how the diffraction features in the vicinity of the ⟨011⟩ directions gradually grow asymmetric with respect to this high-symmetry azimuth. This marked asymmetry is found reproducibly in every one of the four symmetry-equivalent quadrants and therefore cannot be due to any crystal misalignment. The only symmetry-breaking ele-

ment in our experimental setup is the x-ray tube, which is mounted outside the plane defined by the azimuthal rotation axis and the electron-emission direction. We must therefore associate this asymmetry with photon-polarization effects. Even though these experiments have been done using unpolarized x rays, a polarization plane is defined perpendicular to the radiation incidence direction. The photoionization matrix element concentrates flux of primary emission near this plane, which in our geometry is fixed at 41° away from the detection azimuth. Rotating the crystal such that the ⟨011⟩ axes pass through the detection direction, these high-density rows of atoms will move closer to the polarization plane when going from left to right in Fig. 3, i.e., they will experience more primary flux on the right-hand side of each ⟨011⟩ direction in the azimuthal scan. Asymmetric patterns are therefore not unexpected for this experimental geometry. It is, however, quite remarkable that such polarization effects appear to be more important in inelastic than in elastic diffraction.

At first it may be surprising that background intensities show anisotropies of nearly 10%. However, it is well known that Kikuchi electrons, which also have suffered energy losses, produce such patterns.[3] In a sense, the electrons constituting the inelastic tails of XPS core lines can be considered as Kikuchi electrons. At this point, we think that predominantly Bragg-like diffraction features show up in the background diffraction patterns because the geometrical forward-scattering peaks are destroyed by defocusing. The much slower variation with energy loss of the features in the off-symmetry directions indicates that the true short-range diffraction effects in the near-surface emission ($n=0$) already contain some elements of Bragg diffraction off low-index atomic planes that make up the Kikuchi patterns. This had already been seen by Trehan *et al.*[9] and by Osterwalder *et al.*[22] by locating all possible Bragg diffraction directions off low-index planes and associating these with features in XPD patterns from Cu and Ni.

From this we make the general conclusion that XPD patterns contain forward geometrical features, true short-range diffraction, and Bragg diffraction features, where the latter ones can be isolated by an XPD experiment in the background accompanying a core line. Conversely, the XPD patterns of the core line ($n=0$) will often be dominated by geometrical forward features as is evident from Fig. 3. We emphasize that the observed similarity of Auger and Kikuchi electron patterns[11] can hold only if the Kikuchi electrons have experienced small energy losses. In the case of larger energy losses, this equivalence is no longer evident, as shown in the present example. Thus the real distinction in the diffraction patterns from Auger electrons, Kikuchi electrons, and photoelectrons is not by their nature (they all exhibit essentially identical diffraction patterns) but from how deep inside the crystal they originate, meaning how much energy loss they have experienced.

In order to investigate the energy dependence of the phenomena seen in Figs. 2 and 3, we show in Fig. 4 data analogous to those in Fig. 3, which had been obtained with the 2*s* line ($E_{\text{kin}}=1136$ eV), now measured with the

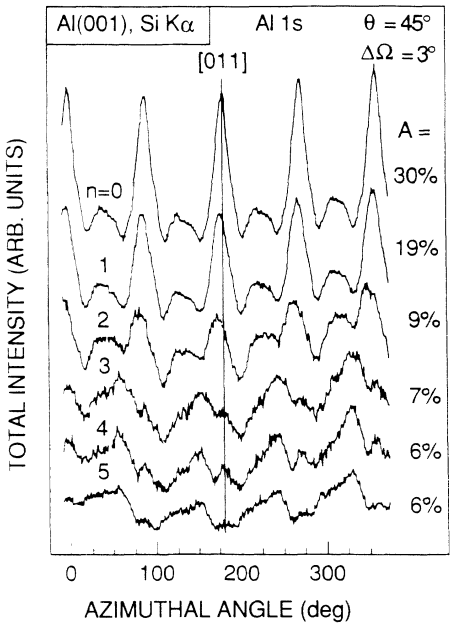

FIG. 4. Same as Fig. 3, however for Si $K\alpha$ excited Al 1*s* emission and associated plasmon-loss peaks.

1*s* line ($E_{\text{kin}}=180$ eV, excited with Si $K\alpha$ radiation). Now the electron mean free path is ≈ 5 Å as compared to 20 Å for the 2*s* photoelectrons. The data in Fig. 4 show the same general trend as those displayed in Fig. 3, with the attenuation of the forward-scattering peaks occurring more or less at the same rate. In view of the very different mean free paths, this observation is somewhat surprising. For each plasmon number n the length of the atomic chain seen along [011] is about four times shorter for the 1*s* case (Fig. 4). This indicates a strong dependence on the electron energy of such defocusing effects. Also, it has to be pointed out that for $n=5$ the inelastically scattered 1*s* photoelectrons have a kinetic energy of only 100 eV. At such a low energy it is well known that forward-scattering effects are very much reduced, even in the absence of defocusing. Note also that in these low-energy data the asymmetry effects relative to the principal crystal axes are much stronger than in the 2*s* case. Again photon-polarization effects are most likely to be the origin of these asymmetries.

As a last example in this series of experiments, we show in Fig. 5 Al 2*s* azimuthal data at a polar angle of $\theta=55°$ off normal. For this polar angle, the azimuthal patterns scan through ⟨111⟩ directions, one of which is indicated in the figure. We see immediately that the forward-scattering features along the ⟨111⟩ directions are not as pronounced as those of the ⟨011⟩ directions. This must be due to the larger interatomic distances in the ⟨111⟩ chains as compared to the ⟨011⟩ chains. We note that the changes with energy separation from the main line ($n=0$) are less drastic in the 55° scan (Fig. 5) than in the 45° scan (Fig. 3). We have suggested above that it is essentially the forward-scattering features that get attenuated when moving the energy window more and more away from the main line into the inelastic back-

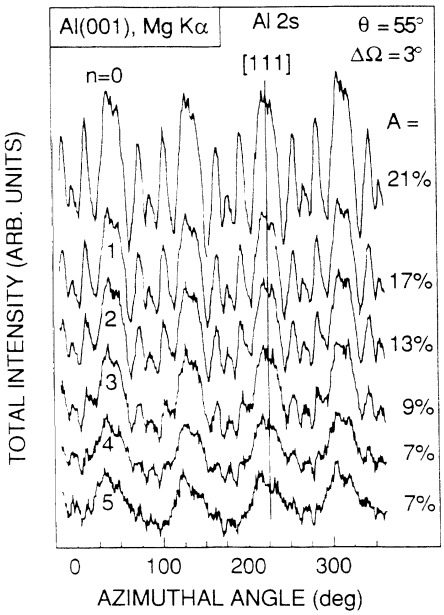

FIG. 5. Same as Fig. 3, however recorded at a polar angle of 55° off normal, including the ⟨111⟩ directions.

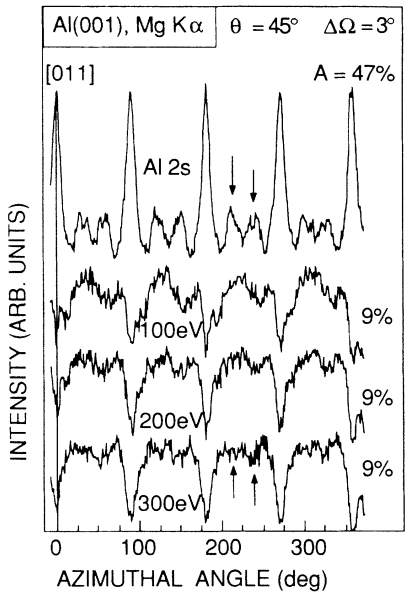

FIG. 6. Azimuthal intensity scans at $\theta=45°$, measured in the Al 2*s* no-loss line ($E_{kin}=1136$ eV) and in the total inelastic background 100, 200, and 300 eV away from the main line, i.e., at kinetic energies of 1036, 936, and 836 eV, respectively. Note that the 300-eV background curve is very nearly the inversion of the no-loss curve, even for the weaker features (see arrows).

ground. Regarding the $\theta=55°$ data in this view, we determine a lack of simple forward-scattering features under these experimental conditions. This finding may also help to understand why the cluster calculations for this polar angle of $\theta=55°$ off normal or 35° off the (001) surfaces of fcc metals have notoriously produced quite poor agreement with the experimental data.[23]

"Electron blocking" along chains of atoms

It was shown in Figs. 2 and 3 that strong defocusing effects take place along chains of atoms in the ⟨011⟩ directions, if the electron-emitting atom is deep enough (≈45 Å) along the row in the crystal. One can then speculate that, if the emitter is even deeper in the crystal along the ⟨011⟩ rows, total destructive interference may take place, which in analogy with ion scattering in crystals one may call "electron blocking." Data to illustrate this effect are shown in Fig. 6. The $\theta=45°$ XPD pattern of the 2*s* line is shown together with azimuthal patterns which have been measured at kinetic energies 100, 200, and 300 eV below that of the 2*s* line. Note that the energy scans show an essentially flat background at these kinetic energies. Most of these electrons come from "deep" (more than 100 Å) inside the crystal, with the average distance from the surface increasing with increasing energy distance from the 2*s* main line. The comparison between the XPD pattern of the 2*s* line and that of the background 300 eV away shows that they are very nearly mirror images, as far as the main features are concerned. This very surprising finding means that, while electrons which are created only a few monolayers below the surface and are contained in the main 2*s* line show enhanced intensity along rows of atoms (like the [011] direction in the case in study), electrons which are created far in the crystal (100 Å and more) and which are mostly contained in the background show reduced intensity along these same rows of atoms. The statement found in the literature, which says that photoelectrons, Auger electrons, and Kikuchi electrons exhibit the same sort of diffraction patterns,[11] must therefore be qualified. This is true only if the Kikuchi electrons originate from the same area in space (quite near the surface at the energies we are concerned with here) as the photoelectrons or Auger electrons, i.e., as long as one is dealing with Kikuchi electrons which have only experienced moderate energy losses (not more than ≈50 eV at an initial kinetic energy of 1000 eV).

Diffraction patterns of medium-energy electrons

In order to check the assumption that the electrons in the inelastic tail of the photoelectrons are in essence ordinary Kikuchi electrons, we present in this section the results of medium-energy electron diffraction (MEED) experiments on the same Al(001) crystal, done under the same conditions as the previously described XPD experiments. The scattering angle is 90°, i.e., at a polar angle of 45° we are observing the specular beam. The inset in Fig. 7 shows an energy spectrum measured at specular reflection from the Al(001) surface with a primary electron energy of 1200 eV. It shows the elastic line and well-developed surface and bulk plasmon peaks not very different from the photoemission data in Fig. 1. Of course the surface plasmons are better developed in the electron-scattering experiment, as now the effective escape depth is halved because the electrons have to penetrate and escape the surface.

The scattering patterns measured for $\theta=45°$ with the

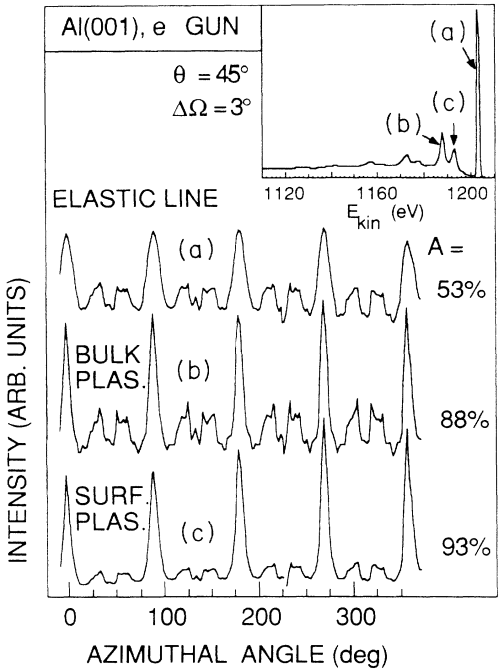

FIG. 7. Azimuthal MEED intensity curves measured at a polar angle of 45° using a primary energy E_p of 1200 eV. Shown are curves measured with the elastic line (a), which in our scattering geometry corresponds to the specular beam, with the first bulk plasmon (b) and with the first surface plasmon (c). The inset gives a corresponding energy scan.

elastic line (*a*) and the first bulk plasmon (*b*) are very similar to those obtained with the 2*s* line and the first bulk plasmon accompanying it (Fig. 3). Only the magnitudes of the anisotropies are different in the two sorts of experiments, with anisotropies of $A=31\%$ and 88% $[A=(I_{\max}-I_{\min})/I_{\max}]$ in the first plasmon-loss curves in XPD and MEED, respectively. Of particular interest is the diffraction pattern of the elastic line (*a*). Except for some changes in the relative intensities of the different features, the elastic MEED pattern is essentially identical to the XPD curves shown in Figs. 2 and 3. Since the elastic line carries a very large intensity under these experimental conditions, such diffraction patterns can be measured with considerable accuracy in very short times, which represents a considerable advantage over conventional XPD. This similarity of MEED and XPD scans has already been observed by Chambers *et al.* in combined MEED and Auger electron-diffraction (AED) experiments on Cu(001) and Ni(001).[6,7] It is very interesting from a theoretical point of view. XPD is generated by exciting a point electron source at a lattice position and subsequent propagation and diffraction to the surface. This picture holds because the 2*s* electrons are quite localized. On the other hand, in the MEED experiment a plane wave of electrons impinges on the surface. The similarity of the two patterns can then be interpreted in the following way: The large momentum transfer perpendicular to the surface, which is needed to reverse the momentum of the MEED electrons, must be provided essentially at the ion cores, where there is enough mass available. Diffraction in the outgoing channel, i.e., after momentum reversal, then dominates the resulting angular intensity patterns. Incident beam diffraction seems to play only a minor role, as has already been discussed by Chambers *et al.*[6,7]

The increase in the anisotropies in going from the elastic line to the first bulk plasmon and the surface plasmon as shown in Fig. 7 is rather surprising and not at all understood. It seems to be associated with variations in the ⟨011⟩ forward-scattering peak intensities mainly, the off-symmetry features more or less conserving their anisotropies. It is therefore likely that multiple scattering along ⟨011⟩ chains is again responsible for this anomalous effect. However, there is no reason for the surface-plasmon diffraction to be different from the elastic-line diffraction, as the probing depth should be essentially the same in the two cases. We can therefore not exclude incident beam effects as being an important factor in determining such surface-plasmon-loss diffraction.

In order to demonstrate as clearly as possible the equivalence of Kikuchi electrons created by photoelectrons and those created in an electron-scattering experiment, Figs. 8 and 9 give a comparison of corresponding diffraction patterns. Figure 8 displays the diffraction patterns at $\theta=45°$ in the first plasmon-loss peak accompanying the 2*s* line excited with Mg $K\alpha$ radiation, and also that same pattern created by the first plasmon peak produced by a beam of 1200 eV electrons. The two diffraction patterns are very similar as expected, with every feature, no matter how small, appearing in both curves and only very minor differences in relative intensities. In Fig. 9 a similar comparison of diffraction patterns is given, measured at $\theta=55°$ off normal and using the second plasmon-loss peak. Again the two patterns are almost identical even for this scan, which includes the very open ⟨111⟩ directions, where multiple-scattering effects have been found to be very important.[23] Note,

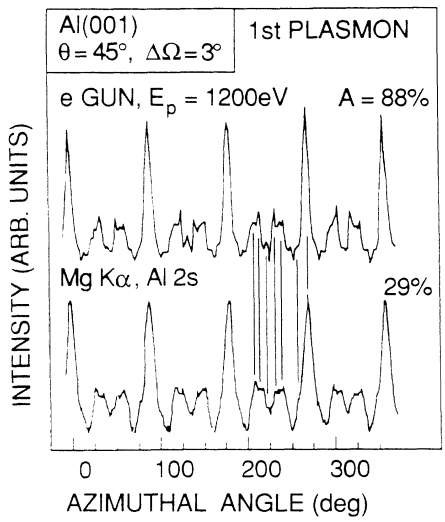

FIG. 8. Comparison of MEED and XPD data from Al(001), measured at $\theta=45°$ in the first bulk plasmon-loss peak. The respective kinetic energies are 1188 and 1121 eV. Vertical lines indicate positions of fine features in the MEED data.

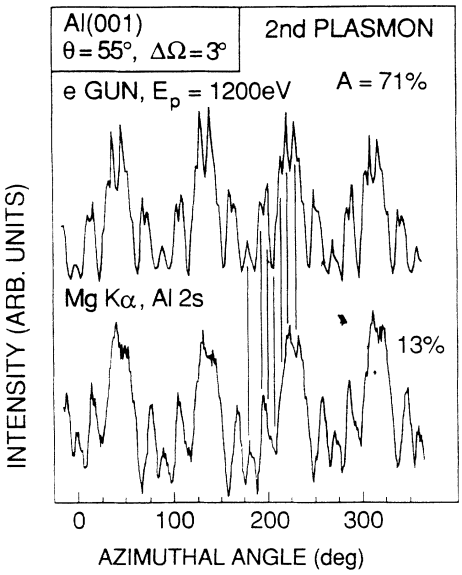

FIG. 9. Same as Fig. 8, however for the second plasmon-loss peak at a polar angle of 55°.

however, that the measuring time for the electron-beam-produced curves is an order of magnitude smaller than that for the XPD pattern.

It is interesting to realize that already at a very early stage of LEED experiments an impressive effort was made to record LEED patterns in a way analogous to our electron-scattering experiments presented here. Gervais *et al.*[24] investigated the scattering of electrons with a kinetic energy between 100 and 1000 eV from a W(110) crystal via rotation of the crystal about its normal (azimuthal scan), while the electron kinetic energy and the polar detection angle were kept constant. Naturally they obtained azimuthal intensity modulations (Renninger plots[25]) of a similar appearance as they are commonplace nowadays in XPD investigations. Even though they extracted no quantitative results from their data, they arrived at some important conclusions. Gervais *et al.*[24] realized that the scattered electron intensity is large in directions of densely packed rows of atoms, and they found that only a dynamical theory could explain their data. These same observations have also been made in recent years with respect to the analysis of substrate XPD experiments. Finally, we mention that Gervais *et al.* also found anisotropies in the distribution of inelastically scattered electrons up to 50 eV away from the primary beam.

CONCLUSION

It has been shown that the inelastic tails accompanying the core lines in a single-crystal photoemission experiment contain considerable angular structure produced by diffraction. This is not unexpected because it only means that the well-known phenomenon of Kikuchi-electron diffraction patterns also show up in XPD experiments. The Kikuchi patterns at losses of a few plasmon energies are different from those of the main line, however, because they do not contain the geometrical forward-scattering features which dominate the core-line XPD patterns under certain geometrical conditions. These differences appear to be related mainly to different depth distributions at which the photoelectrons have been excited, and associated with it the varying degree of multiple scattering. One thus has a convenient tool to separate geometrical forward-scattering features from Bragg-like diffraction features. In particular, at a few hundred eV below a core line, "electron-blocking" effects are observed along densely packed rows of atoms that show enhanced intensities in the core-line XPD.

Finally, a comparison of core-line XPD and electron-diffraction patterns measured at similar kinetic energies is given. Except for the quantitative anisotropies, these patterns are virtually identical, suggesting that substrate XPD patterns should preferably be measured directly in an electron scattering experiment. This is much less time consuming than measuring XPD, possibly more accurate, and allows us to vary the kinetic energy of the electrons freely. This finding is fully consistent with an earlier study by Chambers *et al.*,[6,7] in which they demonstrate further the applicability of MEED to structure determination in thin overlayer systems.

ACKNOWLEDGMENTS

One of the authors (S.H.) acknowledges the hospitality of the Institut de Physique of the Université de Fribourg. This work was supported by the Schweizerischen Nationalfonds.

*Permanent address: Fachbereich Physik, Universität des Saarlandes, Saarbrücken, FRG.

[1]C. S. Fadley, Prog. Surf. Sci. **16**, 275 (1984).
[2]M. Sagurton, E. L. Bullock, and C. S. Fadley, Surf. Sci. **182**, 287 (1987).
[3]H. Hilferink, E. Lang, and K. Heinz, Surf. Sci. **93**, 398 (1980).
[4]W. F. Egelhoff, Jr., Phys. Rev. B **30**, 1052 (1984); S. A. Chambers, H. W. Chen, I. M. Vitomirov, S. B. Anderson, and J. H. Weaver, *ibid.* **33**, 8810 (1986).
[5]M. V. Gomoyunova, I. I. Pronin, and I. A. Shmulevitch, Surf. Sci. **139**, 443 (1984).
[6]S. A. Chambers, I. M. Vitomirov, S. B. Anderson, and J. H. Weaver, Phys. Rev. B **35**, 2490 (1987).
[7]S. A. Chambers, I. M. Vitomirov, and J. H. Weaver, Phys. Rev. B **36**, 3007 (1987).
[8]W. Schaich, Phys. Rev. B **8**, 4078 (1973).
[9]R. Trehan, J. Osterwalder, and C. S. Fadley, J. Electron. Spectrosc. **42**, 187 (1987).
[10]A. Mosser, S. Shindo, and Y. Adachi, Phys. Status Solidi A **43**, 295 (1977); K. Okamoto, T. Ichinokawa, and Y. Ohtsuki, J. Phys. Soc. Jpn. **30**, 1690 (1971).
[11]H. Cronacher, K. Heinz, K. Müller, M. L. Xu, and M. A. Van Hove, Surf. Sci. **209**, 387 (1989).
[12]J. Osterwalder, T. Greber, S. Hüfner, and L. Schlapbach, Phys. Rev. B **41**, 12 495 (1990).
[13]M. L. Xu, J. J. Barton, and M. A. Van Hove, Phys. Rev. B **39**,

8275 (1989).
[14]H. J. Levinson, F. Greuter, and E. W. Plummer, Phys. Rev. B **27**, 727 (1983).
[15]P. Steiner, H. Höchst, and S. Hüfner, Z. Phys. B **30**, 129 (1978).
[16]H. Höchst, P. Steiner, and S. Hüfner, Z. Phys. B **30**, 145 (1978).
[17]H. Raether, in *Excitation of Plasmons and Interband Transitions by Electrons,* Vol. 88 of *Springer Tracts in Modern Physics,* edited by G. Höhler and E. A. Niekisch (Springer, Heidelberg, 1980).
[18]J. Osterwalder, T. Greber, S. Hüfner, and L. Schlapbach, Phys. Rev. Lett. **64**, 2683 (1990).
[19]A. Mosser, Ch. Burggraf, S. Goldsztaub, and Y. H. Ohtsuki, Surf. Sci. **54**, 580 (1976).
[20]S. Y. Tong, H. C. Poon, and D. R. Snider, Phys. Rev. B **32**, 2096 (1985).
[21]C. J. Powell, Surf. Sci. **44**, 29 (1974).
[22]J. Osterwalder, E. A. Stewart, D. Cyr, C. S. Fadley, J. Mustre de Leon, and J. J. Rehr, Phys. Rev. B **35**, 9859 (1987).
[23]J. Osterwalder, A. Stuck, D. J. Friedman, A. Kaduwela, C. S. Fadley, J. Mustre de Leon, and J. J. Rehr, Phys. Scr. (to be published).
[24]A. Gervais, R. M. Stern, and M. Menes, Acta Crystallogr. A **24**, 191 (1968).
[25]M. Renninger, Z. Phys. **106**, 141 (1937).